Supplementary material to the manuscript:

How well do hydrological models simulate streamflow extremes and drought-to-flood transitions?

Eduardo Muñoz-Castro[1,2,3], Bailey J. Anderson[1,2,3], Paul C. Astagneau[1,2,3], Daniel L. Swain[4,5,6], Pablo A. Mendoza[7,8], Manuela I. Brunner[1,2,3]

[1]WSL Institute for Snow and Avalanche Research SLF, Davos Dorf, Switzerland
[2]Climate Change, Extremes and Natural Hazards in Alpine Regions Research Center CERC, Davos Dorf, Switzerland
[3]Institute for Atmospheric and Climate Science, ETH Zurich, Zurich, Switzerland
[4]California Institute for Water Resources, University of California Agriculture and Natural Resources, Davis, CA, USA
[5]Institute of the Environment and Sustainability, University of California, Los Angeles, Los Angeles, CA, USA
[6]Capacity Center for Climate and Weather Extremes, National Center for Atmospheric Research, Boulder, CO, USA
[7]Civil Engineering Department, Universidad de Chile, Santiago, Chile
[8]Advanced Mining Technology Centre (AMTC), Universidad de Chile, Santiago, Chile

Correspondence to: Eduardo Muñoz-Castro (eduardo.munoz-castro@slf.ch)

Contents of this file

This supplementary material file expands on the results of the main manuscript to support - in some cases generalize - and reinforce the findings presented there. The methodology used to generate the data and figures presented here is detailed in the main manuscript. The contents of this file are listed below:

- Figure S12: Results of the ANOVA applied to categorical indices and hydrological variables.
- Figure S13: Correlation between CSI and catchment attributes.
- Figure S14: Parameter agreement for the calibrated model.
- Figure S15: Relative importance of parameters explaining the total variance of the critical the CSI associated with drought, floods, and drought-to-flood transitions.
- Figure S16: Relative importance of bias in hydrological signatures explaining the total variance of the critical success index (CSI) associated with drought, floods, and drought-to-flood transitions.
- Figure S17: Spearman's rank correlation between the relative importance of model parameters and catchment attributes.
- Figure S18: Bias between simulated and observed streamflow extreme events computed at the event scale.
- Table S1: Hydrological signatures computed.
- Table S2: Catchments and configurations with CSI higher than zero for rapid drought-to-flood transitions.

Figure S1: Sensitivity test to explore the role of the threshold used to define droughts and floods in the number of events per year.

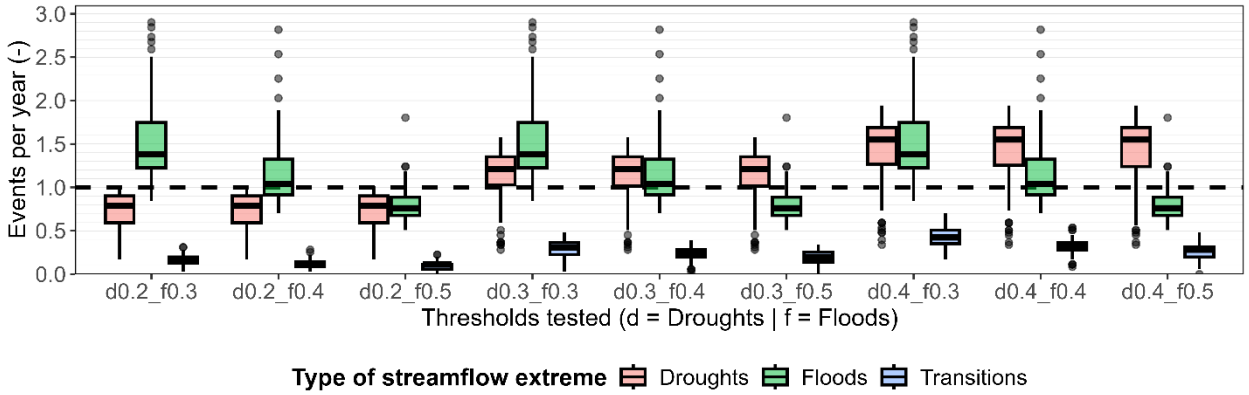

Figure S1: Number of events per year depending on the threshold used for the definition of droughts and floods. The notation "dX_fY" refers to the use of the Xth and Yth percentile to define the variable and fixed threshold required to identify streamflow droughts (d) and floods (f) respectively.

Figure S2: Sensitivity test to explore the effect of the threshold used to define droughts and floods in the model's performance detecting streamflow extreme events.

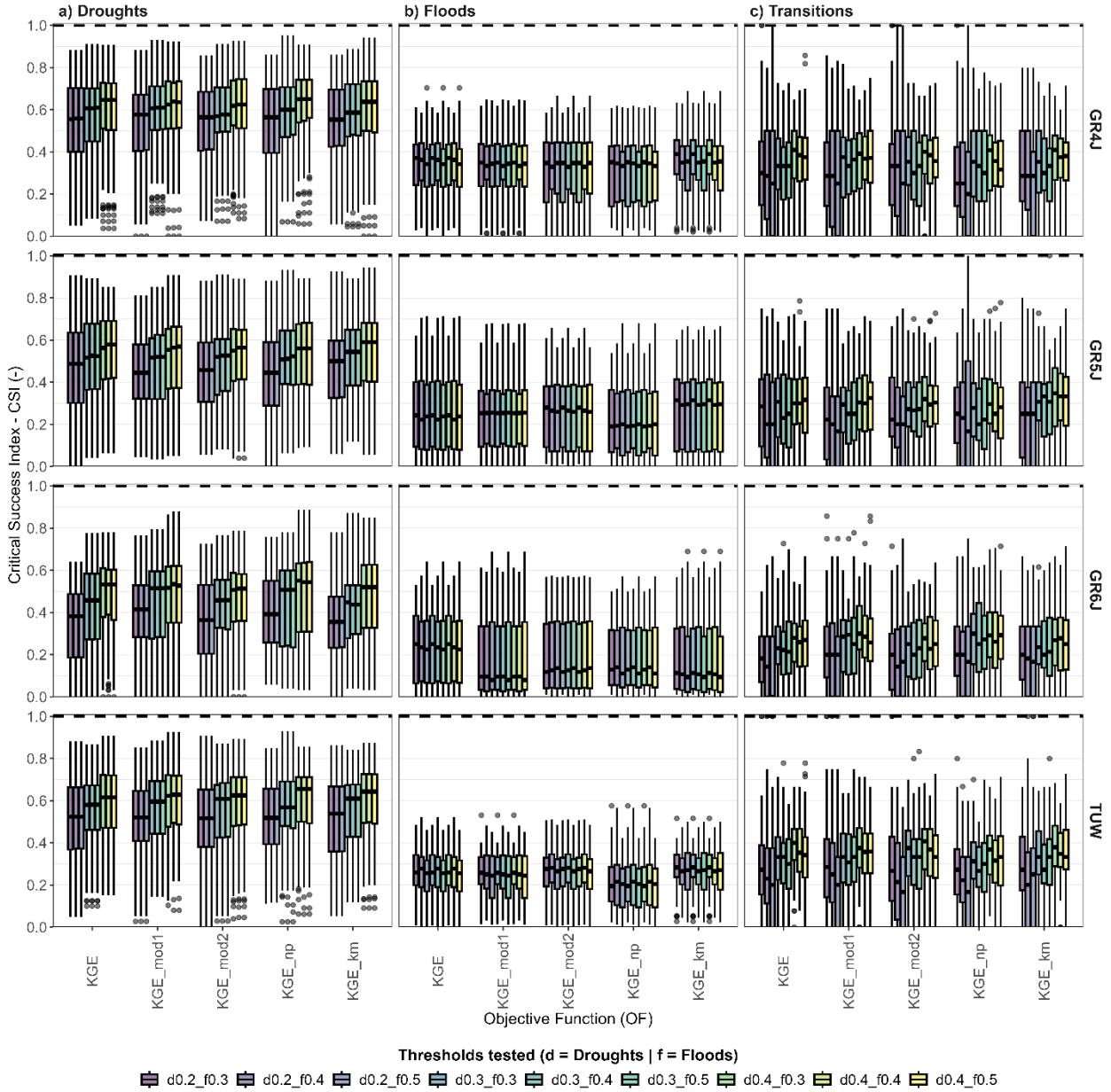

Figure S2: Performance of the GR4J, GR5J, GR6J and TUW models (in the rows) detecting a) droughts, b) floods, and c) transitions, according to different thresholds used for the identification of streamflow extreme events. For each type of extreme event and hydrological model, the results are compared according to different formulations of KGE (unweighted and HiLo) used as objective functions.

Figure S3: Difference in the CSI by putting no weights (reference) and different weights (alternative) on the variability term of the KGE for different hydrological models

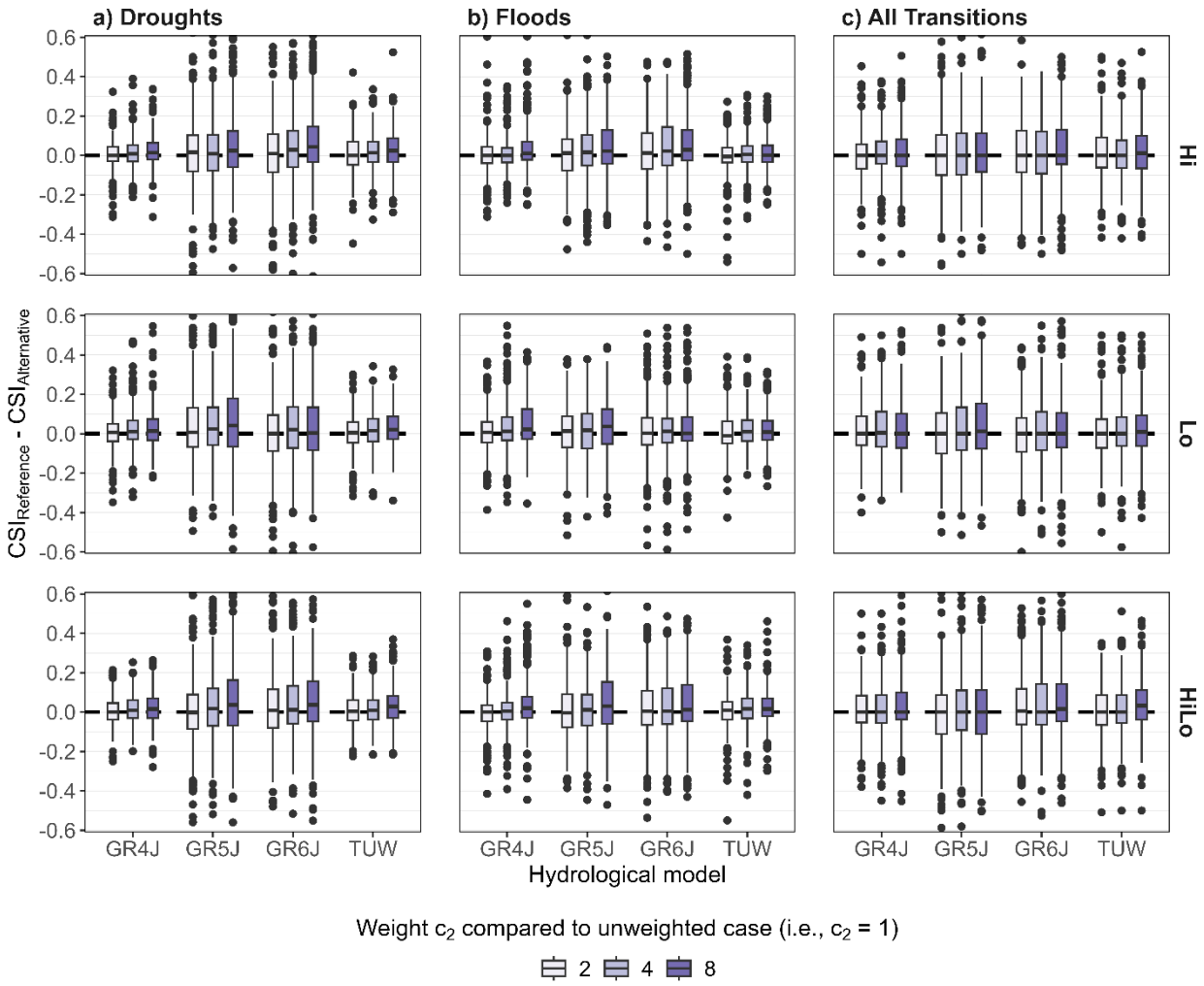

Figure S3: Difference in the Critical Success Index (CSI) for simulations using model calibrations with no weights (reference) versus different weights (alternative) on the KGE variability term for a) droughts, b) floods, and c) transitions. Each alternative is compared with its unweighted analog. Differences are calculated as "reference - alternative" with values above (below) 0 indicating better (worse) performance of the reference (alternative). Supplementary figure associated to Figure 5a in the main manuscript.

Figure S4: Difference in the CSI by using no weights HiLo case (reference) and different weights (alternative) on the variability term of the KGE for different hydrological models

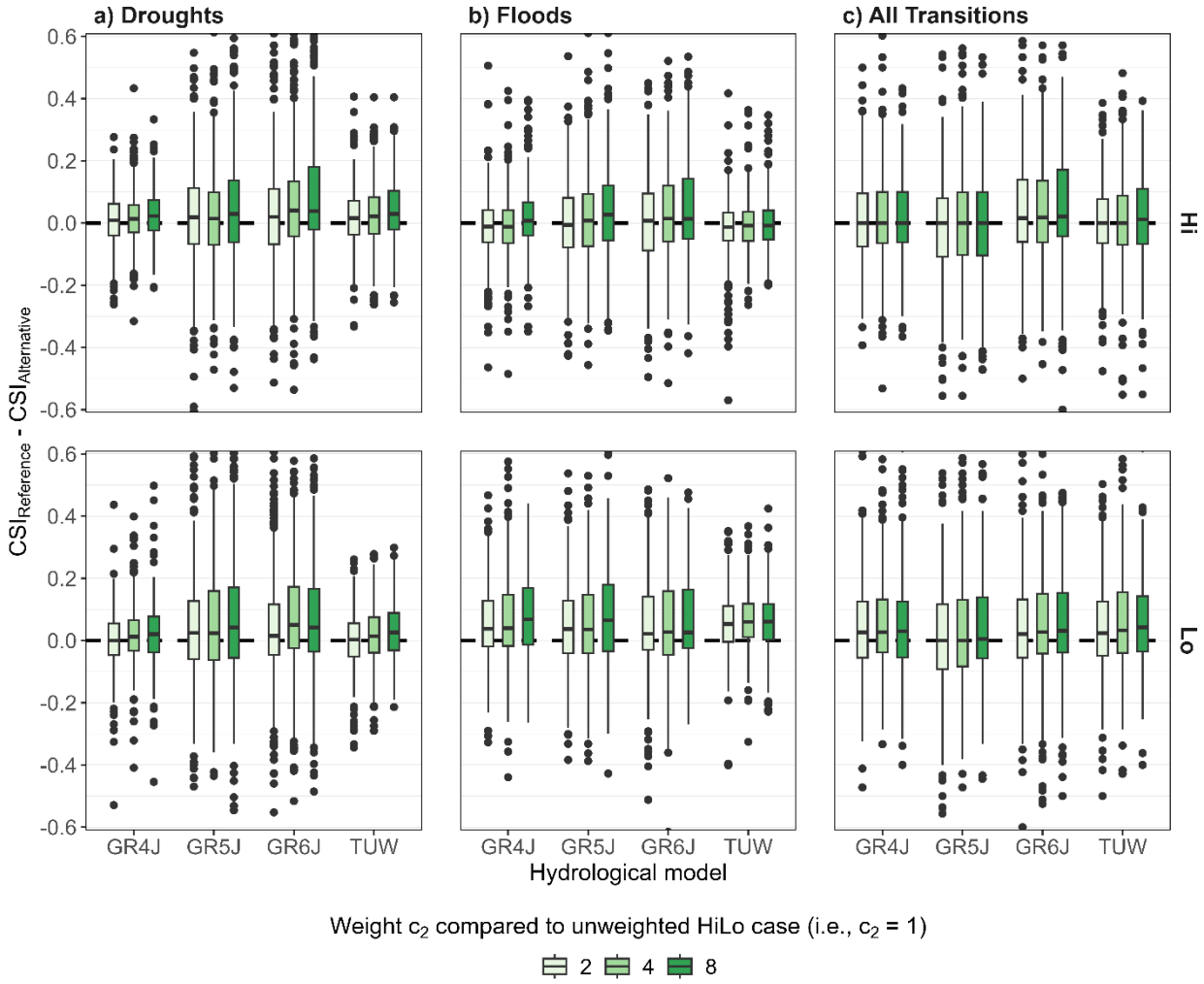

Figure S4: Difference in the Critical Success Index (CSI) for simulations using model calibrations with no weights and HiLo transformation (reference) versus different weights and streamflow transformations (alternative) for a) droughts, b) floods, and c) transitions. Each alternative is compared with its unweighted analogs and HiLo transformation. Differences are calculated as "reference - alternative" with values above (below) 0 indicating better (worse) performance of the reference (alternative). Supplementary figure associated to Figure 5b in the main manuscript.

Figure S5: Spearman's rank correlation coefficient between catchment attributes and ΔCSI for weighted cases with respect to the unweighted reference

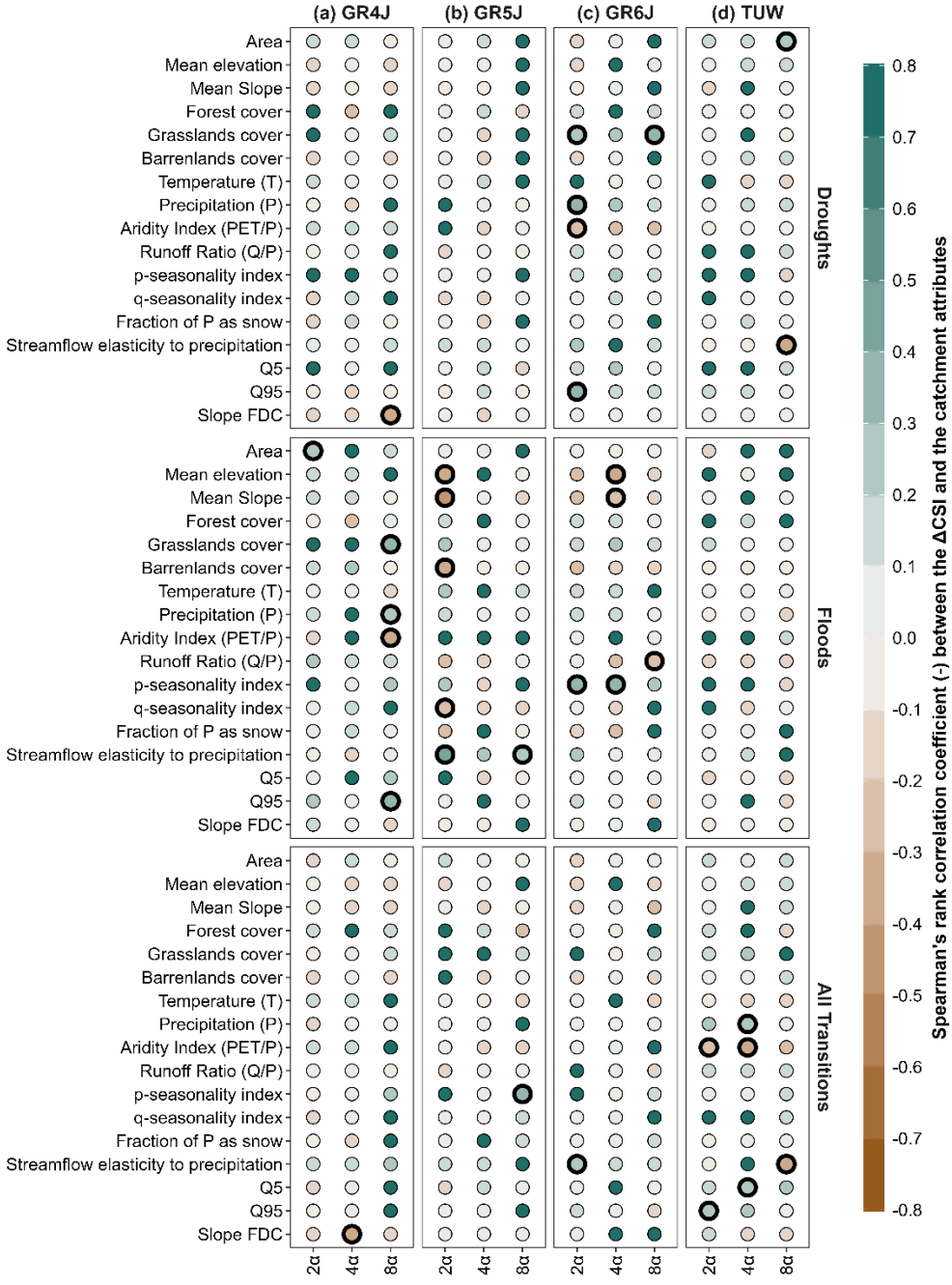

Figure S5: Spearman's rank correlation coefficient between catchment attributes and ΔCSI in detecting droughts, floods, and drought-to-flood transitions (rows) when weights are used in the HiLo original KGE formulations to calibrate the (a) GR4J, (b) GR5J, (c) GR6J, (d) TUW hydrological models (columns). The circles with thick outlines indicate statistically significant correlation coefficients at a 5% level. Positive correlations indicate that the greater the values of the attribute, the unweight case is better in comparison with the alternatives (i.e., use of weights; x-axis).

Figure S6: Performance by using no weights HiLo case with different KGE formulation as objective function for calibration

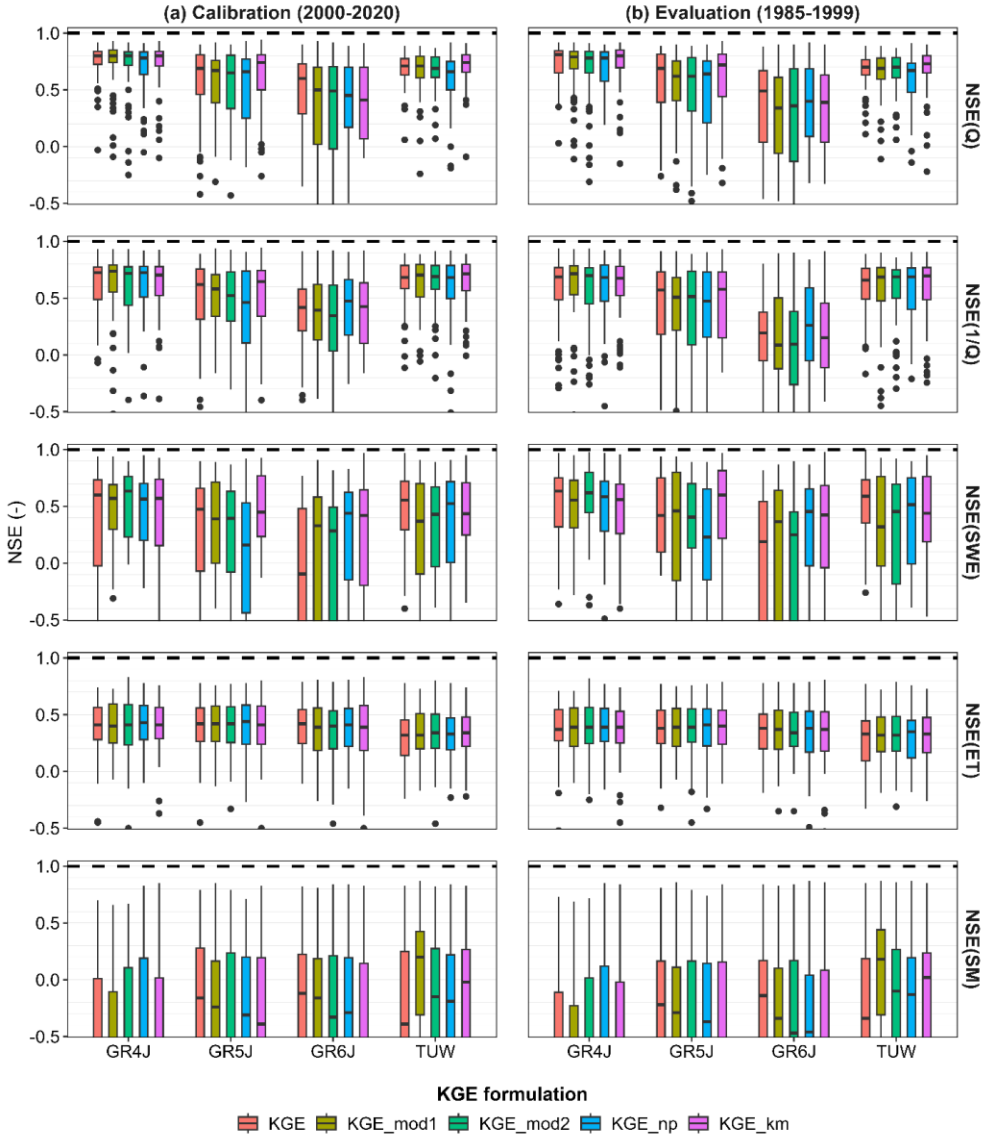

Figure S6: NSE computes for high and low flows (i.e., Q and 1/Q), snow water equivalent (SWE), actual evapotranspiration (ET), and surface soil moisture (SM) for the (a) calibration, and (b) evaluation period. The modeling results are associated with the GR4J, GR5J, GR6J, and TUW hydrological models calibrated using no weights Hilo case and different KGE formulations (used as reference in the main manuscript). The dashed black line represents the optimum value for the assessed metric.

Figure S7: Bias in hydrological signatures by using no weights HiLo case with different KGE formulation as objective function for calibration

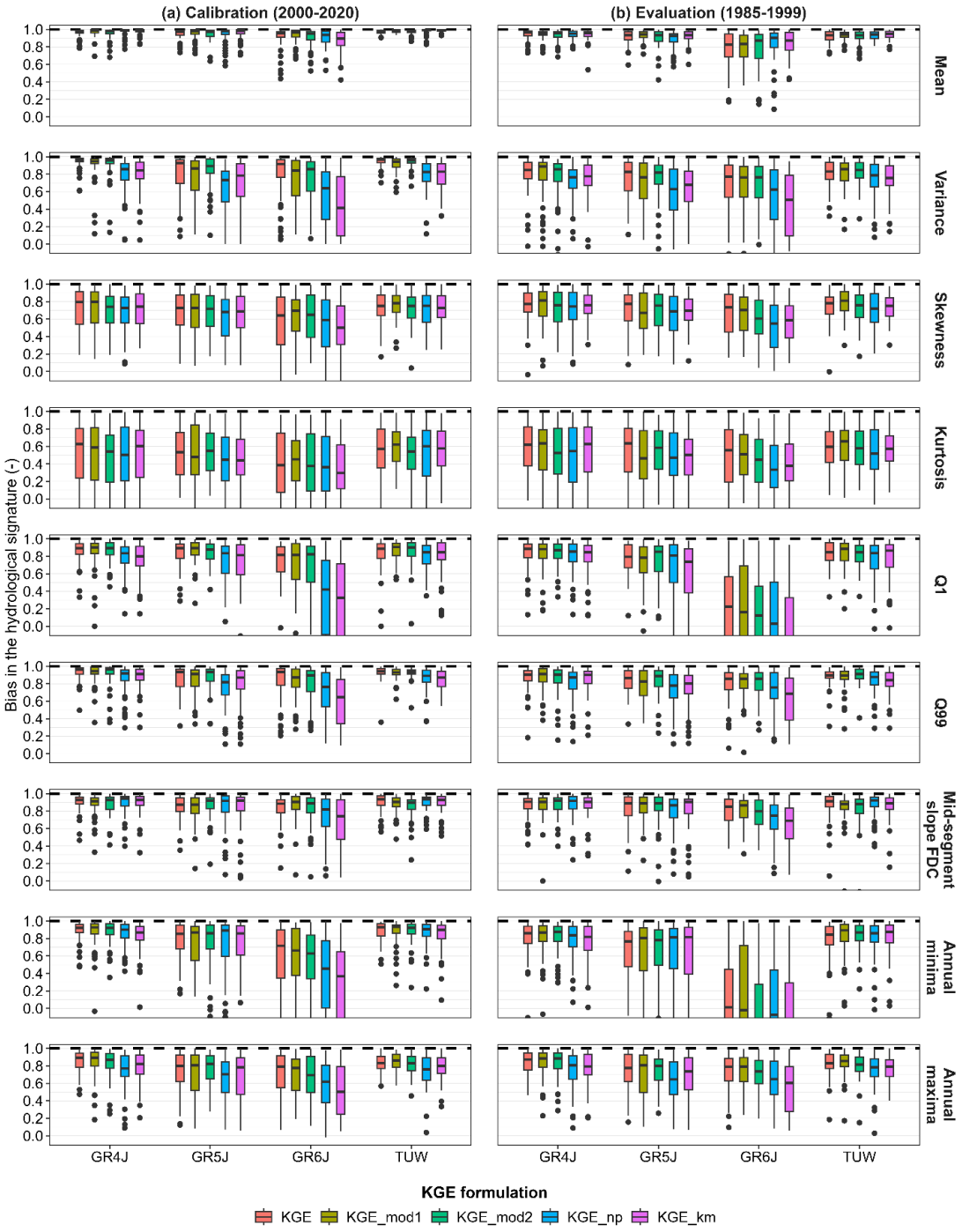

Figure S7: Bias in hydrological signatures computes for streamflow for the (a) calibration and (b) evaluation period. The modeling results are associated with the GR4J, GR5J, GR6J, and TUW hydrological models calibrated using no weights Hilo case and different KGE formulations (used as reference in the main manuscript). The dashed black lines represent the optimum values for the assessed metrics.

Figure S8: Correlation between observed and simulated variables using no weights HiLo case with different KGE formulation as objective function for calibration

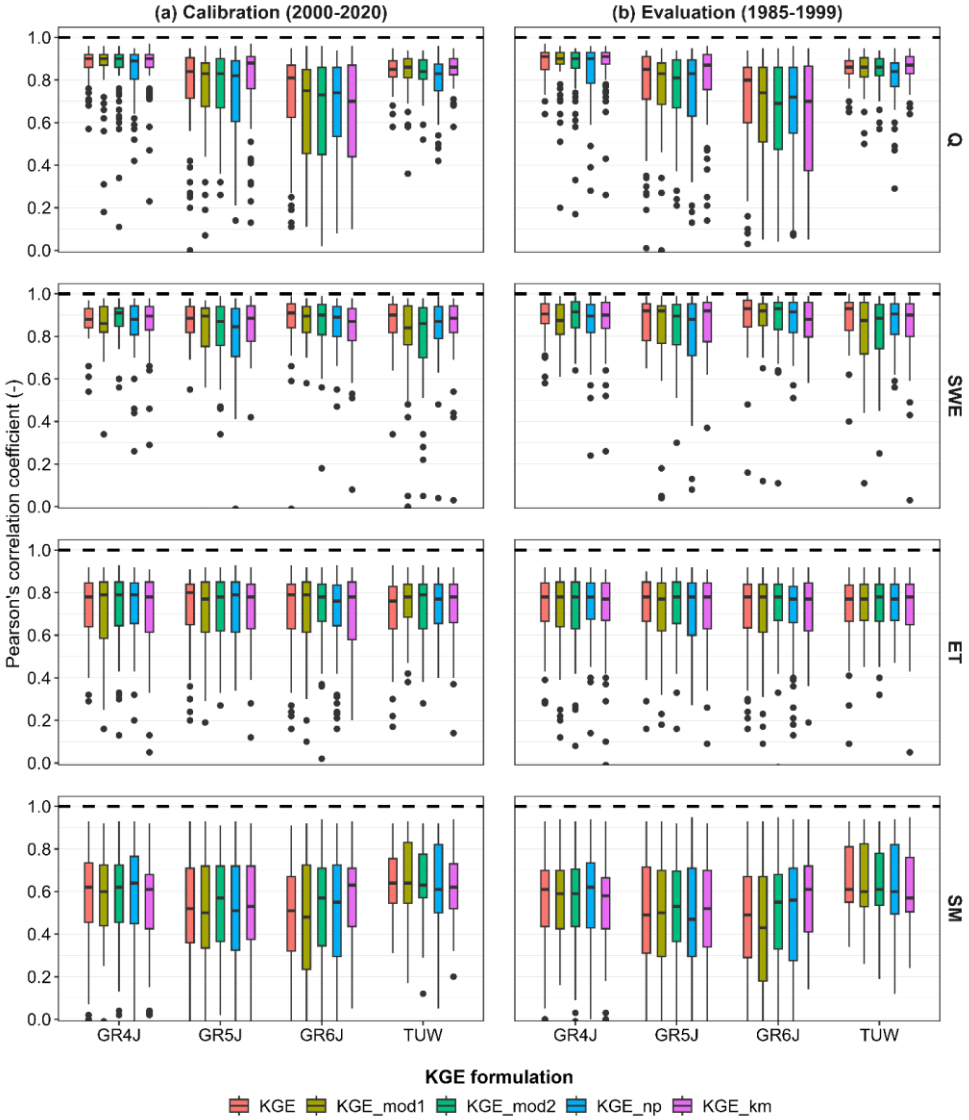

Figure S8: Pearson's correlation coefficient between observed and simulated streamflow (Q), snow water equivalent (SWE), actual evapotranspiration (ET), and surface soil moisture (SM) computed for the (a) calibration and (b) evaluation period. The modeling results are associated with the GR4J, GR5J, GR6J, and TUW hydrological models calibrated using no weights Hilo case and different KGE formulations (used as reference in the main manuscript). The dashed black lines represent the optimum values for the assessed metrics.

Figure S9: Difference in the CSI by using no weights HiLo case (reference) and different weights and streamflow transformations (alternative) for different hydrological models

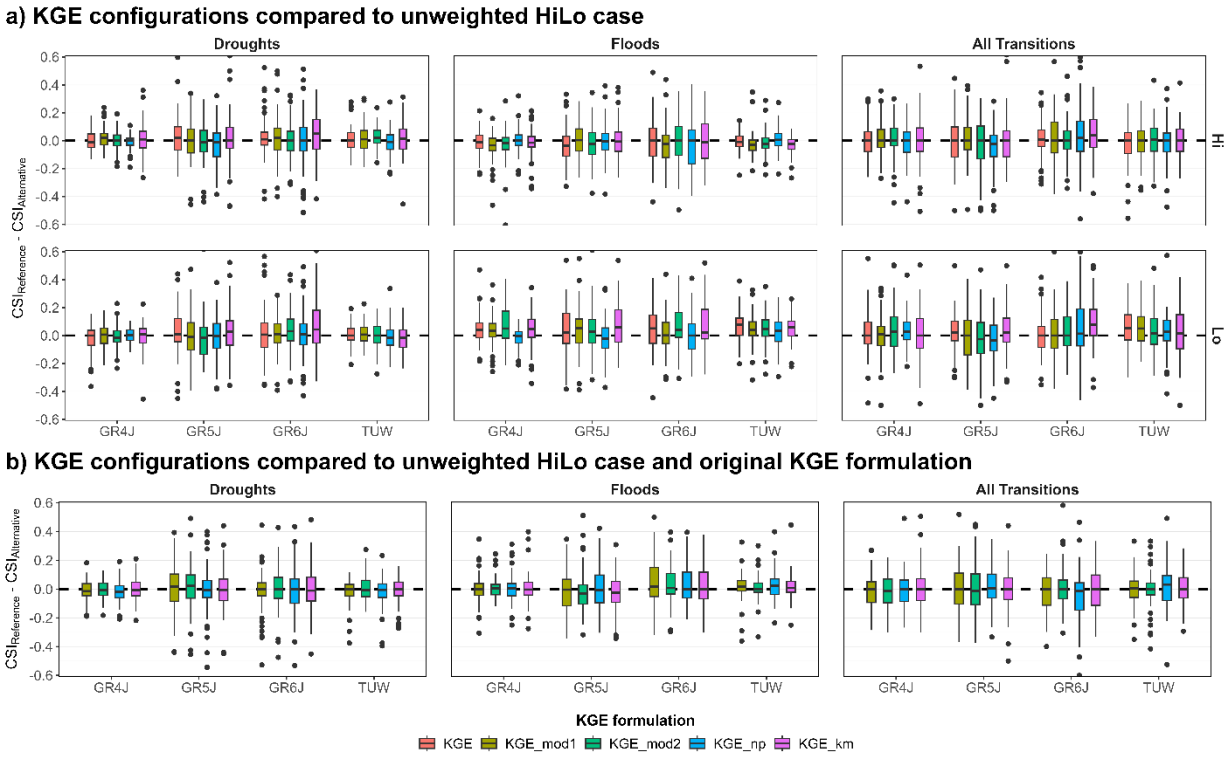

Figure S9: Difference in the Critical Success Index (CSI) for simulations given no weights and HiLo streamflow transformation (reference) and the application of differences weights and streamflow transformation (alternative). In a) each alternative is compared with its unweighted HiLo analogue, while in b) comparisons include both unweighted HiLo analogs and the original KGE formulation as reference. The difference has been calculated as "reference - alternative" which means that values higher (lower) than 0 represent a better (worst) performance of the reference (alternative) simulating high-flows (NSE(Q)), low-flows (NSE(1/Q)), snow water equivalent (NSE(SWE)), actual evapotranspiration (NSE(ET)), and surface soil moisture (NSE(SM)). Supplementary figure associated to Figure 6 in the main manuscript.

Figure S10: Difference in the NSE by using no weights HiLo case (reference) and different weights and streamflow transformations (alternative) for different hydrological models

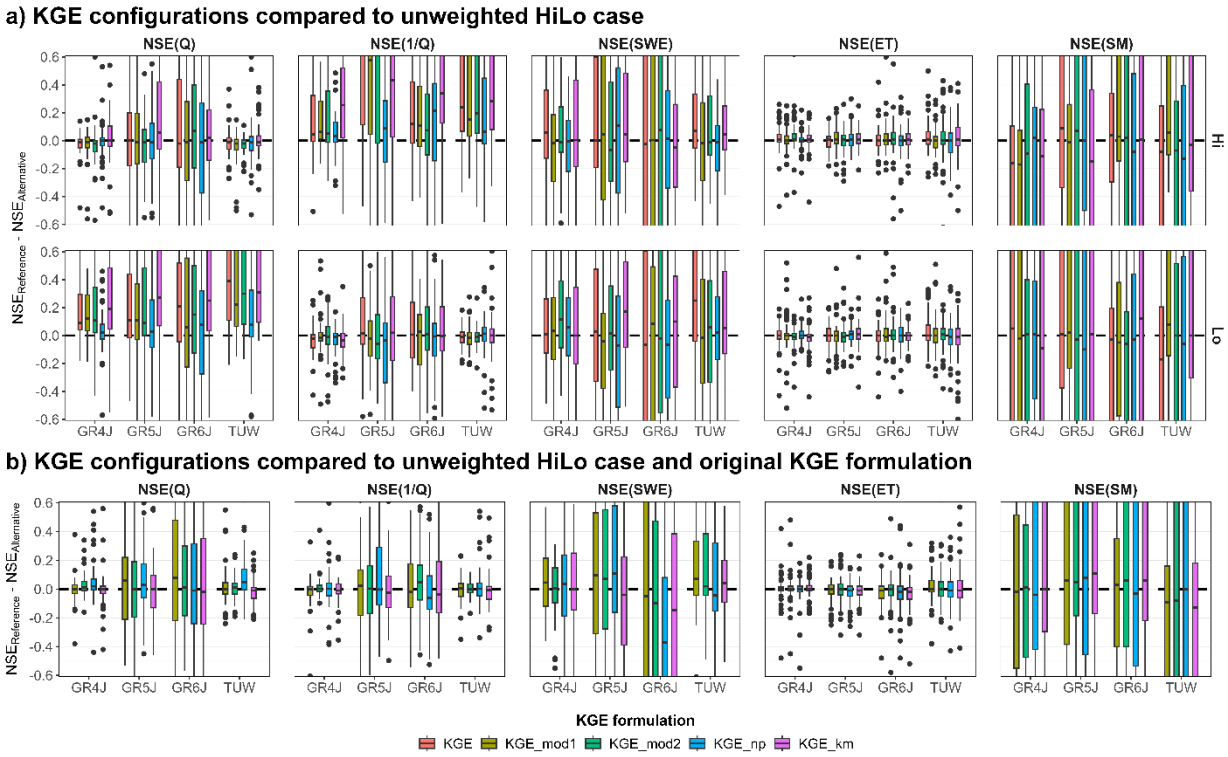

Figure S10: Difference in the Nash-Sutcliffe Efficiency (NSE) for simulations given no weights and HiLo streamflow transformation (reference) and the application of differences weights and streamflow transformation (alternative). In a) each alternative is compared with its unweighted HiLo analogue, while in b) comparisons include both unweighted HiLo analogs and the original KGE formulation as reference. The difference has been calculated as "reference - alternative" which means that values higher (lower) than 0 represent a better (worst) performance of the reference (alternative) simulating high-flows (NSE(Q)), low-flows (NSE(1/Q)), snow water equivalent (NSE(SWE)), actual evapotranspiration (NSE(ET)), and surface soil moisture (NSE(SM)). Supplementary figure associated to Figure 6 in the main manuscript.

Figure S11: CSI per streamflow extreme, objective function, hydrological model and country

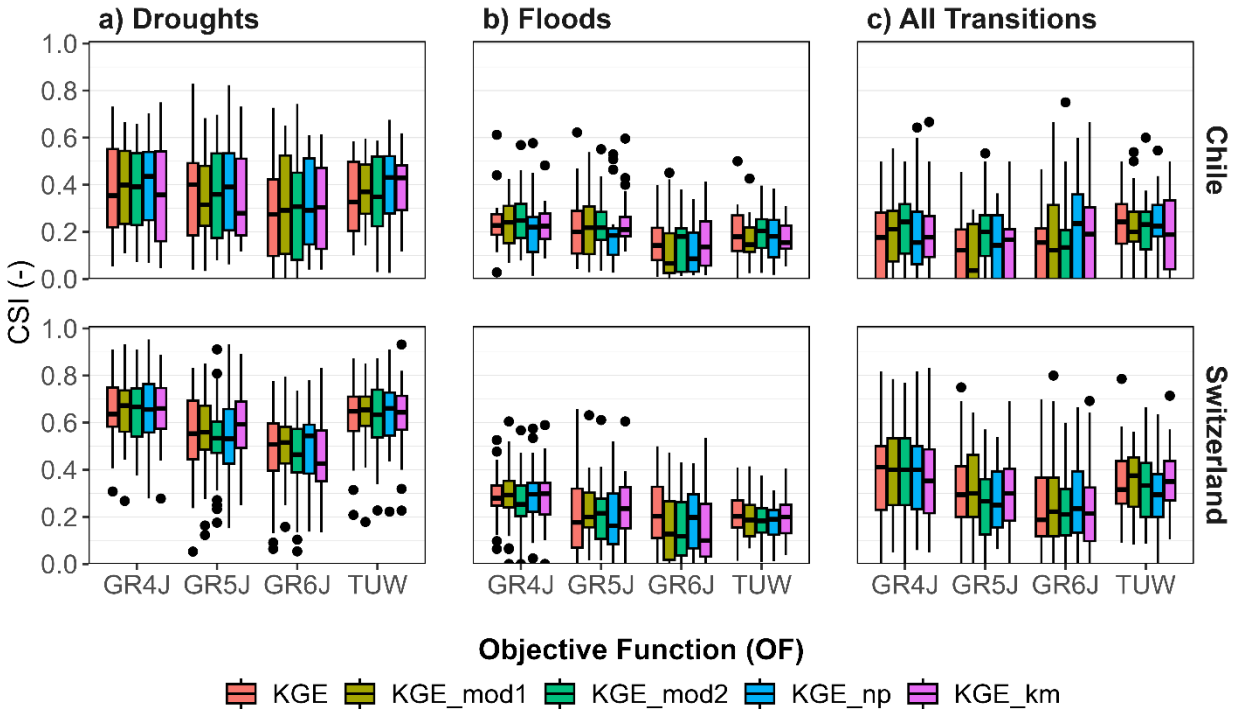

Figure S11: Critical Success Index (CSI) for a) droughts, b) floods, and c) drought-to-flood transitions, based on the simulations with GR4J, GR5J, GR6J, and TUW calibrated with different unweighted HiLo KGE formulations as objective functions for Chile and Switzerland (upper and lower panels respectively). Supplementary figure associated to Figure 7 in the main manuscript.

Figure S12: Results of the ANOVA applied to categorical indices and hydrological variables

a) Results of the ANOVA applied to the categorical indices for streamflow extremes

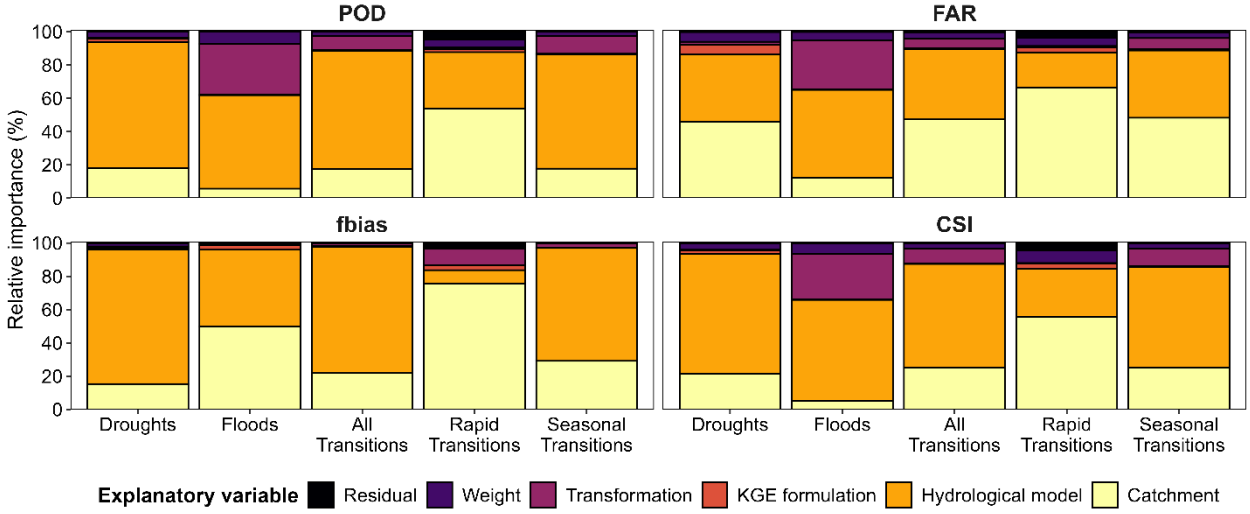

b) Results of the ANOVA applied to the NSE associate to different hydrological variables

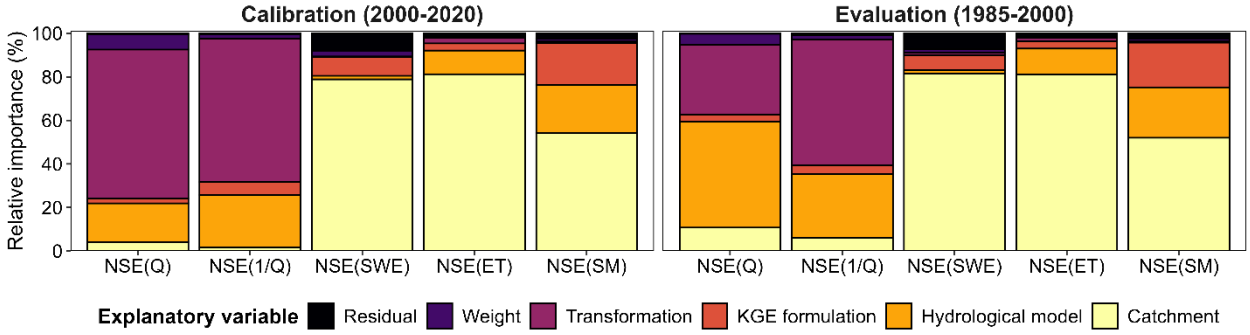

Figure S12: Results of the analysis of variance (ANOVA) applied to a) probability of detection (POD = H/H+M), false alarm ratio (FAR=F/H+F), frequency bias (fbias = H+F/H+M), critical success index (CSI=H/H+M+F) for droughts, floods, all drought-flood transitions (i.e., rapid and seasonal), rapid transitions, and seasonal transitions, and b) the Nash-Sutcliffe Efficiency (NSE) associate to high and low-flows (Q and 1/Q respectively), snow water equivalent (SWE), actual evapotranspiration (ET), and surface soil moisture (SM). Supplementary figure associated to Figure 10 in the main manuscript.

Figure S13: Correlation between CSI and catchment attributes

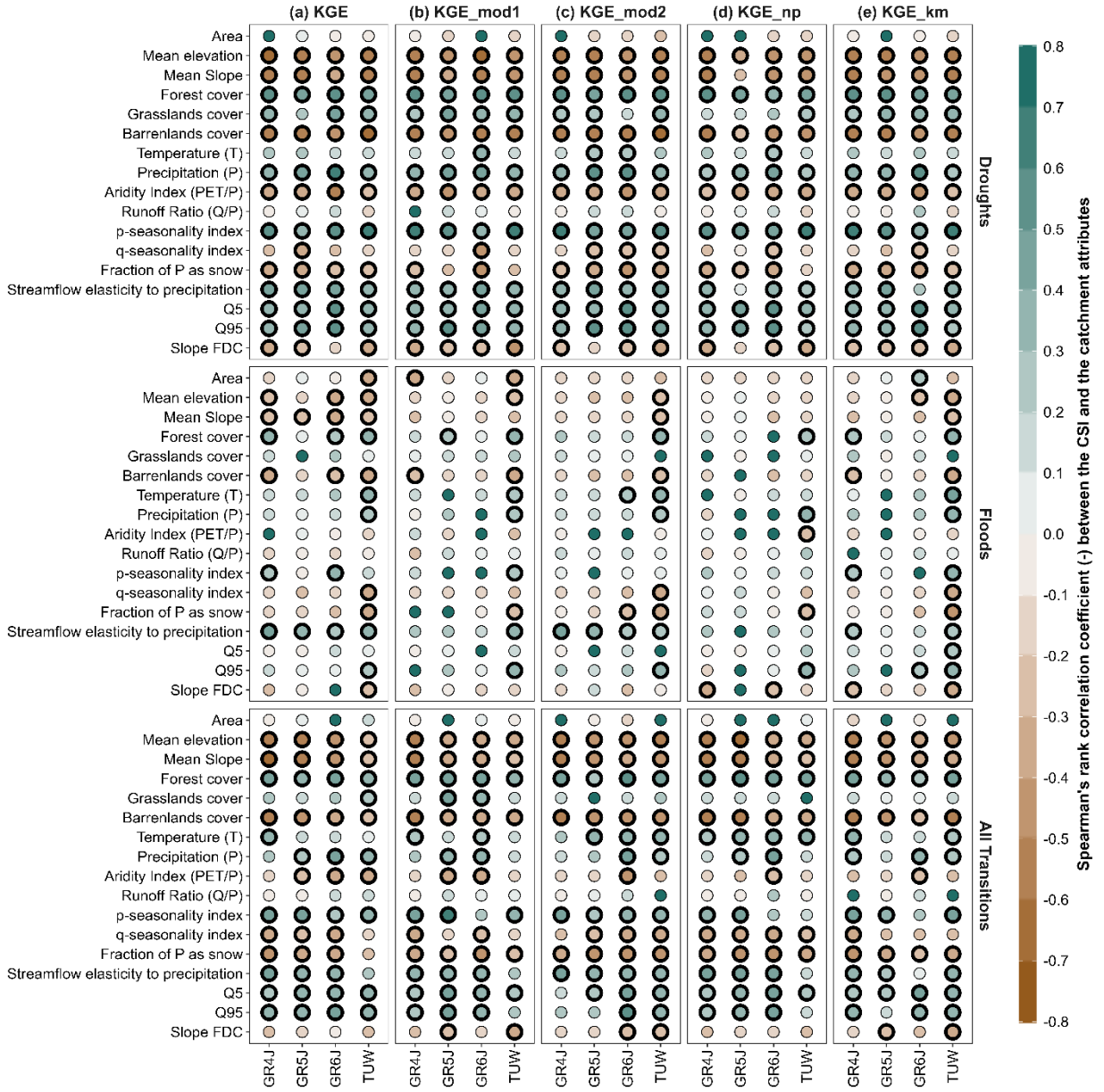

Figure S13: Correlation between CSI and catchment attributes based on results associated to different unweighted HiLo KGE formulations used as objective functions (columns) and streamflow extremes (rows). Supplementary figure associated to Figure 9 in the main manuscript.

Figure S14: Parameter agreement for the calibrated model.

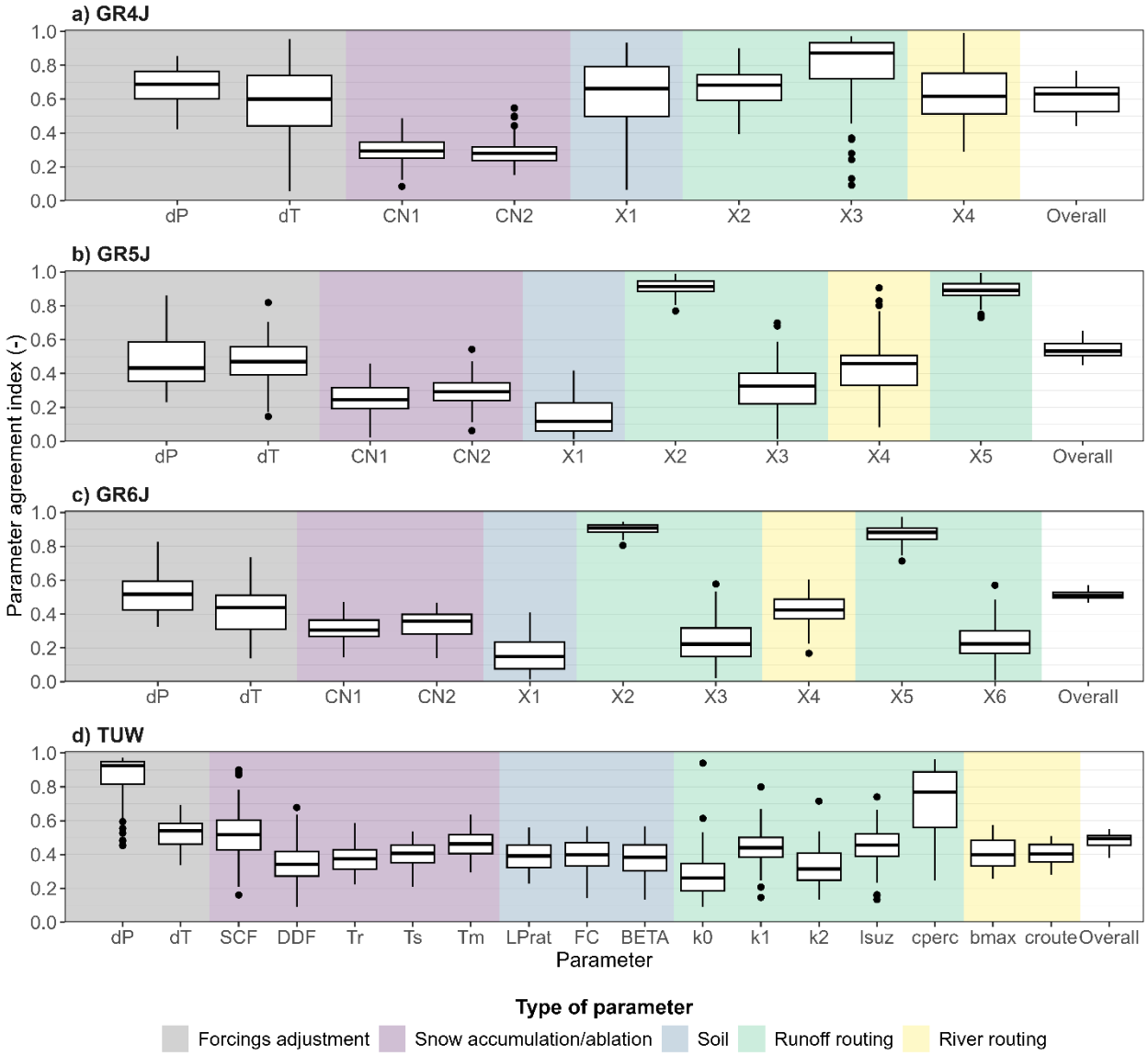

Figure S14: Parameter agreement in a) GR4J, b) GR5J, c) GR6J, and d) TUW models. (Lower) Higher values in the parameter agreement index indicates (dis)agreement in the values of the parameter (i.e., more dispersion between the optimal parameter sets obtained from different calibration processes). Each boxplot comprises agreement indices from the 63 catchments included in the study domain. The parameter agreement index for each parameter and catchment – as well as the overall agreement index - has been computed using the metric proposed by Muñoz-Castro et al. (2023)[1].

[1] Muñoz-Castro, E., Mendoza, P. A., Vásquez, N., & Vargas, X. (2023). Exploring parameter (dis) agreement due to calibration metric selection in conceptual rainfall–runoff models. Hydrological Sciences Journal, 68(12), 1754-1768.

Figure S15: Relative importance of parameters explaining the total variance of the critical the CSI associated with drought, floods, and drought-to-flood transitions

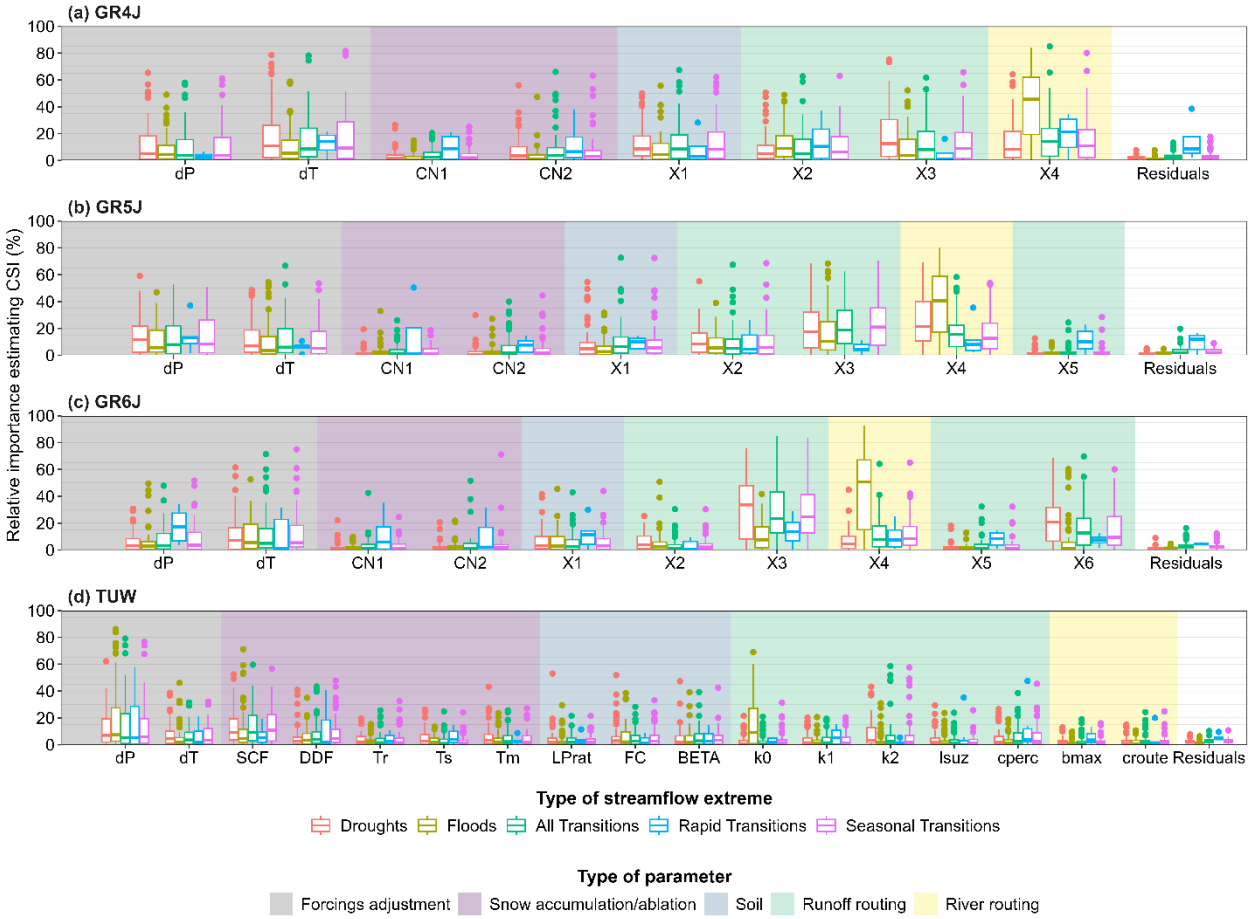

Figure S15: Relative importance of parameters for explaining the Critical Success Index (CSI) for models (a) GR4J, (b) GR5J, (c) GR6J, and (d) TUW based on the results of an analysis of variance (ANOVA). Extended version of Figure 11 in the main manuscript.

Figure S16: Relative importance of bias in hydrological signatures explaining the total variance of the critical success index (CSI) associated with drought, floods, and drought-to-flood transitions

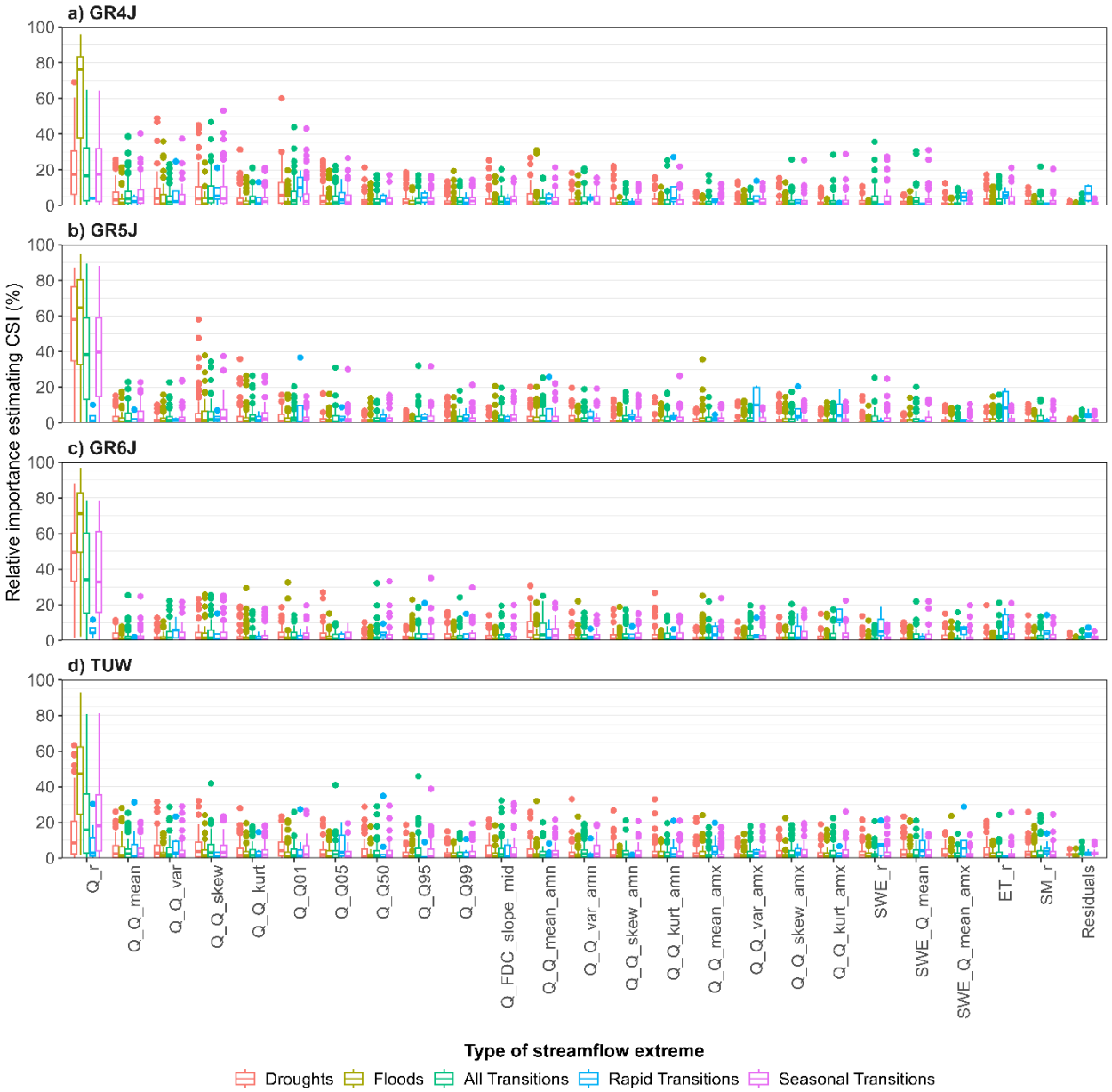

Figure S16: Relative importance of bias in hydrological signatures explaining the total variance of the critical success index (CSI) associated with drought, floods, and drought-to-flood transitions. Q, SWE, ET, and SM represent streamflow, snow water equivalent, actual evapotranspiration, and surface soil moisture respectively. Abbreviations used for the hydrological signatures computed are summarized in Table S1.

Figure S17: Spearman's rank correlation between the relative importance of model parameters and catchment attributes

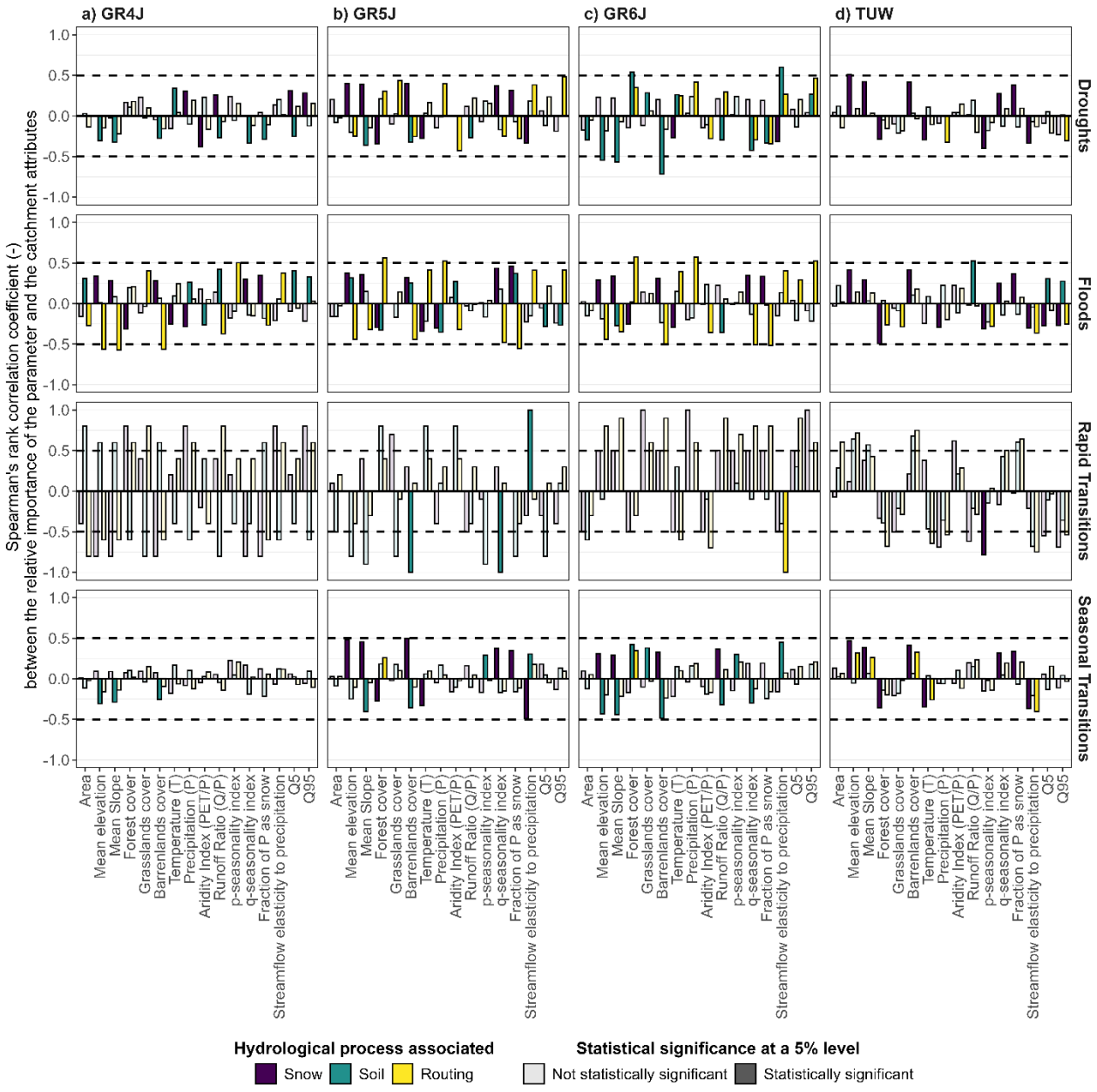

Figure S17: Spearman's rank correlation between the relative importance of model parameters and catchment attributes.

Figure S18: Bias between simulated and observed streamflow extreme events computed at the event scale

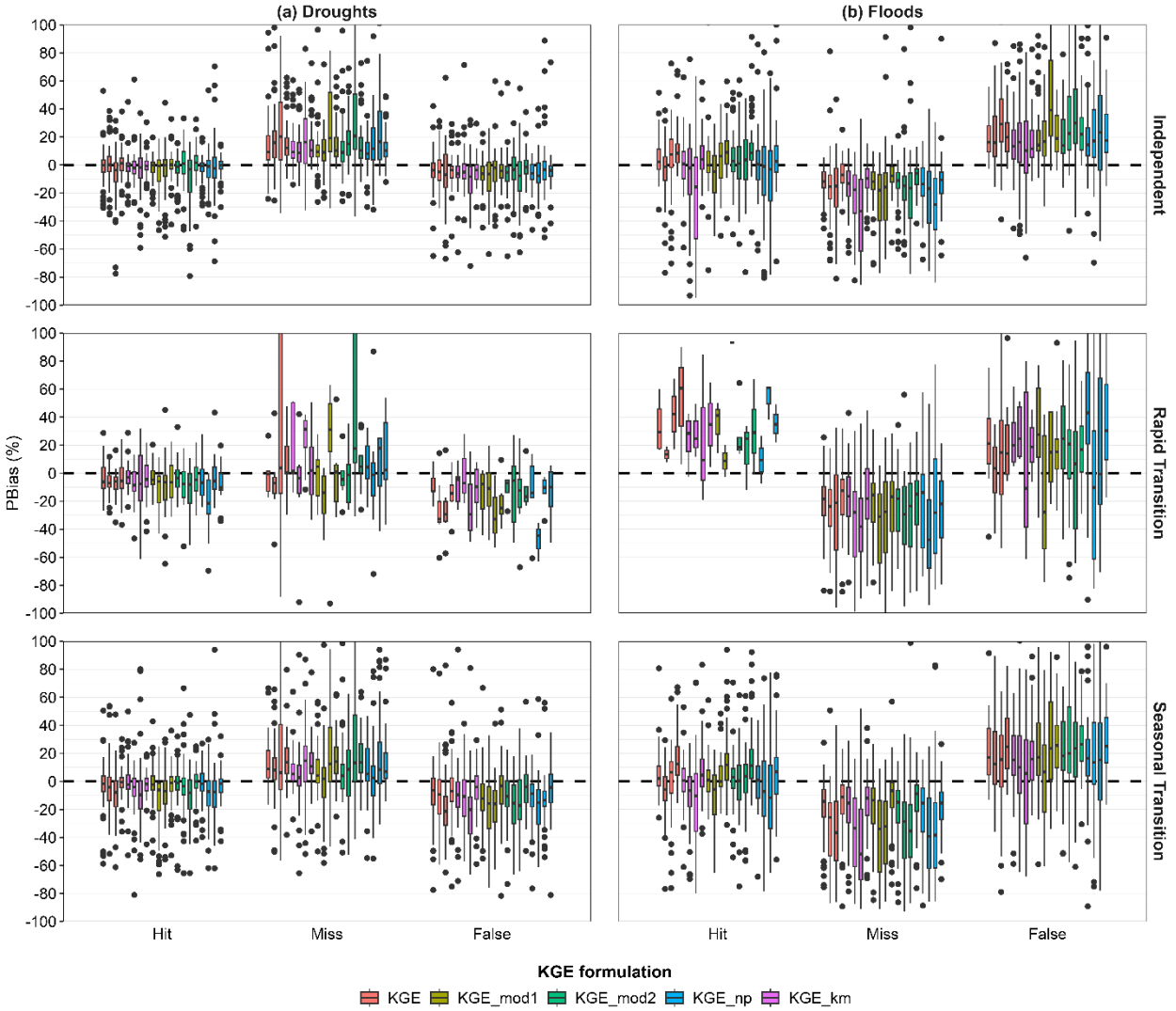

Figure S18: Percentage bias (PBias) between simulated and observed runoff during (a) droughts and (b) floods identified as independent events, rapid transitions, and seasonal transitions, and classified as hit, miss, or false depending on the model's ability to capture them. The modeling results are associated with the GR4J, GR5J, GR6J, and TUW hydrological models calibrated using no weights Hilo case and different KGE formulations (used as reference in the main manuscript). For each KGE formulation there are 4 boxes per category, which correspond to the results obtained for the GR4J, GR5J, GR6J and TUW models respectively. The dashed black lines represent the optimum values for the assessed metrics.

Table S1: Hydrological signatures computed

Table S1: Hydrological signatures computed (used in Figures S7, S8, and S16).

Hydrological signature	**Abbreviation**
Temporal dynamic between observed and simulated values	r
Mean of the daily serie	mean
Variance of the daily serie	var
Skewness of the daily serie	skew
Kurtosis of the daily serie	kurt
1st percentile of the daily serie	Q01
5th percentile of the daily serie	Q05
50th percentile of the daily serie	Q50
95th percentile of the daily serie	Q95
99th percentile of the daily serie	Q99
Slope of the mid-segment of the flow duration curve (FDC)	FDC_slope_mid
Mean of the annual minima serie	mean_amn
Variance of the annual minima serie	var_amn
Skewness of the annual minima serie	skew_amn
Kurtosis of the annual minima serie	kurt_amn
Mean of the annual maxima serie	mean_amx
Variance of the annual maxima serie	var_amx
Skewness of the annual maxima serie	skew_amx
Kurtosis of the annual maxima serie	kurt_amx

Table S2: Catchments and configurations with CSI higher than zero for rapid drought-to-flood transitions

Table S2: Catchments and configurations where CSI values greater than zero are obtained for rapid drought-to-flood transitions. Those corresponding to unweighted HiLo, used as reference in the main manuscript, are highlighted in light blue.

id_gauge	Type	POD	fbias	FAR	CSI	Country	Model	OF_name	Case	w
4311001	Rapid	1.00	2.00	0.50	0.50	Chile	TUW	KGE_np	Hi	1α
	Rapid	1.00	2.00	0.50	0.50	Chile	TUW	KGE_np	HiLo	1α
	Rapid	1.00	2.00	0.50	0.50	Chile	TUW	KGE_np	HiLo	2α
	Rapid	1.00	1.00	0.00	1.00	Chile	TUW	KGE_km	HiLo	2α
	Rapid	1.00	1.00	0.00	1.00	Chile	TUW	KGE_np	Hi	4α
4314002	Rapid	1.00	2.00	0.50	0.50	Chile	TUW	KGE_np	Lo	1α
	Rapid	1.00	3.00	0.67	0.33	Chile	TUW	KGE_mod2	Hi	8α
	Rapid	1.00	1.00	0.00	1.00	Chile	TUW	KGE_km	Lo	8α
	Rapid	1.00	1.00	0.00	1.00	Chile	TUW	KGE_np	HiLo	8α
4320001	Rapid	1.00	3.00	0.67	0.33	Chile	GR4J	KGE_np	Hi	1α
	Rapid	1.00	1.00	0.00	1.00	Chile	GR4J	KGE_mod1	Hi	4α
	Rapid	1.00	1.00	0.00	1.00	Chile	TUW	KGE_mod1	Lo	2α
	Rapid	1.00	1.00	0.00	1.00	Chile	TUW	KGE_km	Lo	2α
	Rapid	1.00	2.00	0.50	0.50	Chile	TUW	KGE_np	Hi	4α
	Rapid	1.00	1.00	0.00	1.00	Chile	TUW	KGE_km	Lo	4α
	Rapid	1.00	3.00	0.67	0.33	Chile	TUW	KGE_mod1	HiLo	8α
5716001	Rapid	1.00	1.00	0.00	1.00	Chile	GR6J	KGE_km	HiLo	4α
	Rapid	1.00	1.00	0.00	1.00	Chile	TUW	KGE_np	Lo	1α
	Rapid	1.00	2.00	0.50	0.50	Chile	TUW	KGE	Lo	2α
	Rapid	1.00	1.00	0.00	1.00	Chile	TUW	KGE_mod1	Lo	2α
	Rapid	1.00	1.00	0.00	1.00	Chile	TUW	KGE_mod2	Lo	2α
	Rapid	1.00	1.00	0.00	1.00	Chile	TUW	KGE_km	Lo	2α
	Rapid	1.00	1.00	0.00	1.00	Chile	TUW	KGE_np	HiLo	2α
	Rapid	1.00	1.00	0.00	1.00	Chile	TUW	KGE_mod2	Lo	8α
	Rapid	1.00	1.00	0.00	1.00	Chile	TUW	KGE_km	Lo	8α
	Rapid	1.00	1.00	0.00	1.00	Chile	TUW	KGE	HiLo	8α
8358001	Rapid	1.00	1.00	0.00	1.00	Chile	GR5J	KGE_km	Hi	8α
	Rapid	1.00	1.00	0.00	1.00	Chile	GR6J	KGE	Hi	8α
	Rapid	1.00	1.00	0.00	1.00	Chile	TUW	KGE	Lo	2α
9104001	Rapid	1.00	1.00	0.00	1.00	Chile	GR4J	KGE	HiLo	1α
	Rapid	1.00	1.00	0.00	1.00	Chile	GR4J	KGE_mod2	HiLo	2α
	Rapid	1.00	1.00	0.00	1.00	Chile	GR4J	KGE	HiLo	4α
	Rapid	1.00	1.00	0.00	1.00	Chile	GR4J	KGE_mod2	HiLo	4α
	Rapid	1.00	1.00	0.00	1.00	Chile	GR4J	KGE	HiLo	8α
	Rapid	1.00	1.00	0.00	1.00	Chile	GR5J	KGE_mod2	Lo	8α
	Rapid	1.00	1.00	0.00	1.00	Chile	TUW	KGE_mod1	Lo	2α
	Rapid	1.00	2.00	0.50	0.50	Chile	TUW	KGE	Lo	4α
	Rapid	1.00	2.00	0.50	0.50	Chile	TUW	KGE	Lo	8α
	Rapid	1.00	1.00	0.00	1.00	Chile	TUW	KGE_mod2	Lo	8α
	Rapid	1.00	1.00	0.00	1.00	Chile	TUW	KGE_np	Lo	8α

id_gauge	Type	POD	fbias	FAR	CSI	Country	Model	OF_name	Case	w
	Rapid	1.00	1.00	0.00	1.00	Chile	TUW	KGE_mod1	HiLo	8α
9127001	Rapid	1.00	2.00	0.50	0.50	Chile	TUW	KGE_km	HiLo	4α
2606	Rapid	0.50	0.50	0.00	0.50	Switzerland	GR4J	KGE_mod2	HiLo	1α
2151	Rapid	1.00	3.00	0.67	0.33	Switzerland	GR5J	KGE_mod2	Lo	2α
2029	Rapid	1.00	3.00	0.67	0.33	Switzerland	GR5J	KGE_mod1	Hi	4α
	Rapid	1.00	1.00	0.00	1.00	Switzerland	GR5J	KGE_mod2	Lo	4α
	Rapid	1.00	3.00	0.67	0.33	Switzerland	GR5J	KGE_mod1	Lo	8α
	Rapid	1.00	1.00	0.00	1.00	Switzerland	GR5J	KGE_km	Lo	8α
	Rapid	1.00	1.00	0.00	1.00	Switzerland	GR5J	KGE_mod1	HiLo	8α
	Rapid	1.00	3.00	0.67	0.33	Switzerland	GR6J	KGE	Hi	1α
	Rapid	1.00	1.00	0.00	1.00	Switzerland	GR6J	KGE_np	Lo	2α
	Rapid	1.00	1.00	0.00	1.00	Switzerland	GR6J	KGE_mod1	Hi	8α
	Rapid	1.00	2.00	0.50	0.50	Switzerland	GR6J	KGE_mod2	HiLo	8α
2110	Rapid	1.00	2.00	0.50	0.50	Switzerland	TUW	KGE_km	Hi	8α
2099	Rapid	0.50	1.00	0.50	0.33	Switzerland	GR6J	KGE	Hi	2α
2018	Rapid	0.50	0.50	0.00	0.50	Switzerland	GR4J	KGE_km	Hi	1α
	Rapid	0.50	0.50	0.00	0.50	Switzerland	GR4J	KGE	Hi	2α
	Rapid	0.50	0.50	0.00	0.50	Switzerland	GR4J	KGE_mod2	Hi	2α
	Rapid	0.50	0.50	0.00	0.50	Switzerland	GR4J	KGE_km	Hi	2α
	Rapid	0.50	0.50	0.00	0.50	Switzerland	GR4J	KGE_mod1	HiLo	4α
	Rapid	0.50	0.50	0.00	0.50	Switzerland	GR5J	KGE	Hi	1α
	Rapid	0.50	0.50	0.00	0.50	Switzerland	GR5J	KGE_mod2	Hi	4α
	Rapid	0.50	0.50	0.00	0.50	Switzerland	GR5J	KGE_km	Hi	8α
	Rapid	0.50	0.50	0.00	0.50	Switzerland	GR5J	KGE_mod1	Lo	8α
	Rapid	0.50	1.00	0.50	0.33	Switzerland	GR6J	KGE_mod2	Lo	1α
	Rapid	0.50	0.50	0.00	0.50	Switzerland	GR6J	KGE_km	Hi	2α
	Rapid	0.50	1.50	0.67	0.25	Switzerland	GR6J	KGE	HiLo	2α
	Rapid	0.50	0.50	0.00	0.50	Switzerland	GR6J	KGE_mod2	Hi	4α
	Rapid	0.50	1.00	0.50	0.33	Switzerland	GR6J	KGE_np	Hi	4α
	Rapid	0.50	0.50	0.00	0.50	Switzerland	GR6J	KGE_km	Hi	4α
	Rapid	1.00	1.50	0.33	0.67	Switzerland	GR6J	KGE_np	Hi	8α
	Rapid	0.50	1.00	0.50	0.33	Switzerland	GR6J	KGE	HiLo	8α
	Rapid	0.50	1.50	0.67	0.25	Switzerland	TUW	KGE_mod1	Hi	1α
	Rapid	0.50	0.50	0.00	0.50	Switzerland	TUW	KGE_mod2	Hi	1α
	Rapid	0.50	1.00	0.50	0.33	Switzerland	TUW	KGE_np	Hi	1α
	Rapid	0.50	1.00	0.50	0.33	Switzerland	TUW	KGE_np	Lo	1α
	Rapid	1.00	1.50	0.33	0.67	Switzerland	TUW	KGE_np	HiLo	1α
	Rapid	1.00	1.00	0.00	1.00	Switzerland	TUW	KGE_km	HiLo	1α
	Rapid	0.50	1.00	0.50	0.33	Switzerland	TUW	KGE	Hi	2α
	Rapid	0.50	1.50	0.67	0.25	Switzerland	TUW	KGE_mod2	Hi	2α
	Rapid	1.00	1.00	0.00	1.00	Switzerland	TUW	KGE_np	Hi	2α
	Rapid	0.50	0.50	0.00	0.50	Switzerland	TUW	KGE_km	Hi	2α
	Rapid	0.50	0.50	0.00	0.50	Switzerland	TUW	KGE	Lo	2α
	Rapid	0.50	0.50	0.00	0.50	Switzerland	TUW	KGE_mod1	Lo	2α
	Rapid	0.50	0.50	0.00	0.50	Switzerland	TUW	KGE_mod2	Lo	2α
	Rapid	0.50	0.50	0.00	0.50	Switzerland	TUW	KGE_np	Lo	2α

id_gauge	Type	POD	fbias	FAR	CSI	Country	Model	OF_name	Case	w
	Rapid	0.50	1.00	0.50	0.33	Switzerland	TUW	KGE_km	Lo	2α
	Rapid	0.50	1.00	0.50	0.33	Switzerland	TUW	KGE_km	HiLo	2α
	Rapid	0.50	1.00	0.50	0.33	Switzerland	TUW	KGE	Hi	4α
	Rapid	0.50	0.50	0.00	0.50	Switzerland	TUW	KGE_mod1	Hi	4α
	Rapid	0.50	1.00	0.50	0.33	Switzerland	TUW	KGE_mod2	Hi	4α
	Rapid	0.50	0.50	0.00	0.50	Switzerland	TUW	KGE_np	Hi	4α
	Rapid	0.50	1.50	0.67	0.25	Switzerland	TUW	KGE_km	Hi	4α
	Rapid	0.50	1.00	0.50	0.33	Switzerland	TUW	KGE_mod1	Lo	4α
	Rapid	0.50	0.50	0.00	0.50	Switzerland	TUW	KGE_np	Lo	4α
	Rapid	0.50	0.50	0.00	0.50	Switzerland	TUW	KGE	HiLo	4α
	Rapid	0.50	1.00	0.50	0.33	Switzerland	TUW	KGE_mod2	HiLo	4α
	Rapid	0.50	1.00	0.50	0.33	Switzerland	TUW	KGE	Lo	8α
	Rapid	0.50	0.50	0.00	0.50	Switzerland	TUW	KGE_mod1	HiLo	8α
	Rapid	0.50	0.50	0.00	0.50	Switzerland	TUW	KGE_mod2	HiLo	8α
	Rapid	0.50	0.50	0.00	0.50	Switzerland	TUW	KGE_km	HiLo	8α